American Journal of Physics

NOTES AND DISCUSSIONS | SEPTEMBER 01 2022

Comment on "A study of the longitudinal laser modes of a semiconductor laser using optical coherence tomography" [Am. J. Phys. 75, 569–571 (2006)]

Abdulaziz M. Aljalal

Am. J. Phys. 90, 715–717 (2022)
https://doi.org/10.1119/5.0090620

Comment on "A study of the longitudinal laser modes of a semiconductor laser using optical coherence tomography" [Am. J. Phys. 75, 569–571 (2006)]

Abdulaziz M. Aljalal[a)]
Physics Department, King Fahd University of Petroleum and Minerals, Dhahran, Saudi Arabia

(Received 8 March 2022; accepted 28 June 2022)

Although the longitudinal mode spacing and longitudinal mode widths of a typical laser diode can, in principle, be determined from an optical coherence tomography signal, the values presented by Poddar *et al.* [Am. J. Phys. **75**, 569–571 (2006)] do not agree with the Fourier transform theory. Also, the mode spacing is inconsistent with the peak separation in the interference signal. Moreover, the laser cavity mirror reflectivity calculated from the laser spectrum is incorrect because it ignores the gain and the loss within the laser cavity. This Comment aims to help readers who may struggle to understand that paper or to reproduce its results.
https://doi.org/10.1119/5.0090620

Poddar *et al.* published a paper in this journal about using optical coherence tomography to study the longitudinal modes of a diode laser.[1] However, the paper lacked sufficient detail to help readers understand how to implement similar measurements in their own labs and may have contained some errors in measurement or analysis. Toward the goal of helping the reader avoid possible mistakes in similar setups, this article comments on three topics presented in the paper: obtaining a resolved spectrum for the longitudinal modes of the laser, measuring the power–current curve of the laser, and extracting reflectivity of the cavity mirrors from the width of a longitudinal mode spectrum.

An optical coherence tomography apparatus is usually used for imaging. It employs a Michelson interferometer with a broadband light source such as a superluminescent diode. In a Michelson interferometer, an incoming light beam from a light source is split into two beams that are reflected back by two mirrors to recombine at the beam splitter and interfere. The optical path difference between the two interfering beams can be adjusted by translating either of the two mirrors. Since the light beam passes twice in each arm, the optical path difference is twice the length difference between the two arms. The broadband light source has a short longitudinal coherence length, and the Michelson interferometer produces an interference signal only when its two arms differ in length by less than a few coherence lengths. In time-domain optical coherence tomography, a sample replaces the mirror in one arm of the interferometer, and the length of the other arm is varied to image the sample. A reflecting layer in the sample that makes the two arms almost equal in length causes variation in the interferometer's output signal.

To study the longitudinal modes of a diode laser, the experimental apparatus described in Ref. 1 replaced the broadband light source with a diode laser and the sample with a mirror. The interference signal was measured over 16 mm of translation of the mirror of the reference arm of the interferometer. According to the inset in Fig. 5 of that paper, the full width at half maximum of a longitudinal mode is 0.3 GHz, and the difference between two adjacent data points in the frequency domain is 0.03 GHz. However, these numbers contradict the Fourier transform theory, which dictates that the minimum separation between two adjacent points in the frequency domain is $\Delta f = c/2\Delta x_m$, where c is the speed of light and $2\Delta x_m$ is the maximum optical path difference between the two interfering beams. Hence, for $2\Delta x_m = 2 \times 16\,\text{mm}$, $\Delta f = 9\,\text{GHz}$. To obtain $\Delta f = 0.03\,\text{GHz}$, the interference signal should be collected at least over 5 m of translation of the mirror of the reference arm.

Reference 1 provides no details about how the position of the translating mirror shown in the inset e of Fig. 2 is transformed into the frequency domain of Fig. 3. When carefully examining the two figures, it appears that the spectrum has the same shape as the coherence tomography signal, except flipped horizontally. Also, Figs. 3 and 5 in Ref. 1, presumably using the same data points, have different frequency scales. The frequency scale of Fig. 3 is inconsistent with the quoted values for the stated width of curve b (48 GHz) and the mode spacing (14.3 GHz).

The multiple peaks in the interference signal are due to the equally spaced modes of the laser, but they are not the modes in themselves. A spectrum with equally spaced peaks separated by f_{fsr} produces peaks in the interference signal both when the arms are equal and when they differ by an integer multiple of $c/2f_{\text{fsr}}$.[2]

In the following, the output signals of a Michelson interferometer due to a light source with a smooth spectrum and one with equally spaced peaks are modeled and compared. For an input light source that is monochromatic with frequency f and intensity I_0, it is straightforward to show that the intensity of the output signal of the interferometer is

$$I(\Delta x) = I_0\{1 + \cos[2\pi f(2\Delta x)/c]\}. \quad (1)$$

Here, Δx is the length difference between the two arms. Hence, for an input light source, which has an intensity of

$S(f)df$ in the frequency range between f and $f + df$, the output signal is

$$I(\Delta x) = \int_0^\infty S(f)\{1 + \cos[2\pi f(2\Delta x)/c]\}df. \quad (2)$$

The intensity of the light source I_0 is related to the intensity spectral density $S(f)$ by $I_0 = \int_0^\infty S(f)df$.

Figure 1(a) shows a simulated smooth spectrum with a width of Δf and central frequency f_0, while Fig. 1(d) shows a spectrum obtained by multiplying that of Fig. 1(a) by equally spaced identical narrow spectral lines, each of width δf, separated by f_{fsr}. The spectrum of Fig. 1(d) is like a spectrum of a multi-longitudinal mode laser, with the separation between two adjacent modes given by the free spectral range of the laser Fabry–Pérot cavity $f_{\text{fsr}} = c/2L$, where L is the cavity's optical length. Equation (2) can be solved analytically using a Gaussian function for the narrow spectral lines. Figure 1(b) shows the resulting interference pattern when using the spectrum in Fig. 1(a), and Fig. 1(e) shows the interference pattern when using the spectrum in Fig. 1(d). Figure 1(b) shows that for the smooth spectrum, interference occurs only near zero optical path difference with a width of about $c/\Delta f$. In the interference region, the intensity has a modulation wavelength of about $2\Delta x \approx \lambda_0 = c/f_0$, but the sinusoidal variation cannot be resolved using the scale used in the figure. Hence, the interference region appears as a solid painted area. Figure 1(e) shows that for the equally spaced multipeak spectrum of Fig. 1(d), interference not only occurs at zero optical path difference but also for optical path length differences that are integer multiples of c/f_{fsr}. As in Fig. 1(b), the width of the individual interference regions is about $c/\Delta f$. As indicated by the dashed curve in Fig. 1(e), the extent of optical path differences over which interference can occur is inversely proportional to the spectral width of the individual spectral peak, and it is about $c/\delta f$.

In a typical time-domain optical coherence tomography setup, the reference mirror moves at a constant speed v. The motion of the mirror causes the frequency f of the laser beam to be Doppler shifted. If the mirror moves toward the detector, the frequency of the light reflecting from the moving mirror becomes $f' = ((1 + v/c)/(1 - v/c))f \approx (1 + 2(v/c))f = f + 2v/\lambda$. A superposition of the beam reflected by the stationary mirror and the beam reflected by the moving mirror produce a beat whose beat frequency equals the difference between the frequencies of the two beams, $2v/\lambda$. Since the response of optical detectors is much slower than the optical frequencies, their output is proportional to the square of the envelope of the beat signal. Hence, the output signal for the Michelson interferometer has modulation at a frequency of about $2v/\lambda_0$. Heterodyne detection uses this modulation to extract the envelope shown in Figs. 1(c) and 1(f), from the signals in Figs. 1(b) and 1(e). The detected signal is band-passed by a filter whose center frequency is the Doppler shift frequency $2v/\lambda_0$. The output signal is then rectified and low-pass filtered.[3] In Ref. 1, the speed of the translation stage is 0.6 mm/s, and the wavelength of the laser is 670 nm, so the Doppler shift should be 1.8 kHz and not the quoted frequency of 1.4 kHz. For a speed of 0.6 mm/s, a laser with a wavelength of 850 nm would give a Doppler shift of 1.4 kHz.

There is an inconsistency in Ref. 1 between the spacing between peaks in the interference signal and the frequency difference between adjacent laser modes. From the inset of Fig. 2 in Ref. 1, the spacing between peaks in the interference signal is $\Delta x = 1.3$ mm or an optical path difference of $2\Delta x = 2.6$ mm. Thus, the frequency difference between two adjacent laser modes should be $f_{fsr} = c/2\Delta x = 115$ GHz. Reference 1, however, finds it to be 14.3 GHz from its Fig. 5.

There is also an inconsistency between the spacing of the laser modes and the calculated laser length. The two facets of a diode laser form a Fabry–Pérot cavity, and hence, the spacing of its modes f_{fsr} is related to its optical length L by

$$f_{fsr} = \frac{c}{2L}. \quad (3)$$

In the aforementioned formula, the variation of the refractive index with frequency is ignored. Thus, the optical length of the laser when 14.3 GHz is used for the mode spacing should

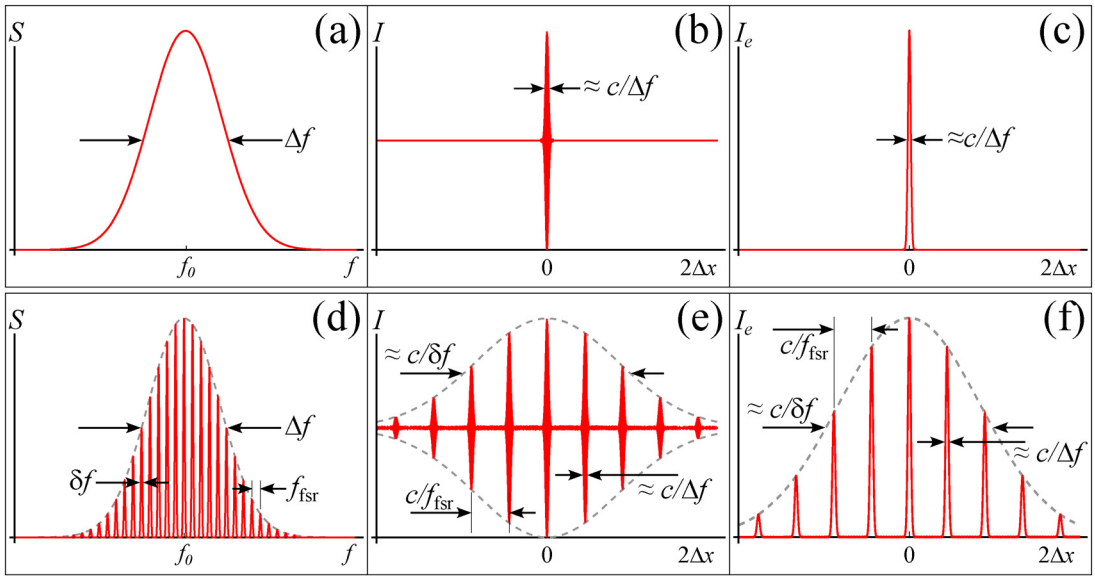

Fig. 1. (a) A smooth intensity spectrum, (b) the interference signal due to a light source with spectrum (a), (c) the envelope of signal (b), (d) a spectrum with equally spaced identical peaks, (e) the interference signal due to a light source with spectrum (d), and (f) the envelope of signal (e).

be $L = c/2f_{fsr} = 10.5$ mm, not 1.064 mm, as quoted in Ref. 1. The optical length corresponding to correct mode spacing $f_{fsr} = 115$ GHz is 1.3 mm, which is the spacing between adjacent interference peaks in the optical coherence tomography signal. If the variation in the refractive index with frequency is considered, Eq. (3) should be

$$f_{fsr} = \frac{c}{2n_g l}. \tag{4}$$

Here, $n_g = n + f dn/df = n - \lambda\, dn/d\lambda$ is the group index of refraction and l is the physical length of the laser cavity.[4] Using Eq. (4) and the physical length 335 μ m obtained from the optical microscope image in Ref. 1 give a group index of refraction $n_g = 3.9$. A 670 nm diode laser is usually made from GaInP/AlGaInP semiconductors.[5] However, since the laser structure and composition are not known, it is difficult to compare the calculated group index of refraction 3.9 with one from literature. For example, the group index of refraction for $(Al_xGa_{1-x})_{0.5}In_{0.5}P$ is from 3.9 to 4.8 for x from 0.9 to 0.1.[6]

Figure 2 in Ref. 1 shows the power vs the injection current. The power is constant at 40 a.u. for currents below 6 mA, increases linearly between 6 and 30 mA, then becomes constant at 260 a.u. for currents above 30 mA. It appears that the detection system is fully saturated beyond an injection current of 30 mA. Although it is clear from the figure that the laser threshold current occurs at 6 mA, Ref. 1 states that the threshold current is beyond 25 mA, close to the current for which the detection system saturation may start to occur. Also, below the threshold current, the optical power should be practically zero compared to the lasering output power. However in Ref. 1, the power below the threshold current is very high. It is 40 a.u. compared to the full scale 260 a.u., which indicates either the detector is not shielded well from the ambient light or the detection system has a dc offset.

If the detection system is sensitive enough, interference in the optical coherence tomography signal should be observed even below the threshold current. For currents well below threshold, the spontaneous emission spectrum of the diode laser is smooth, and it is typically a few nanometers in width. In this case, a peak in the optical coherence tomography signal is observed when the two arms of the Michelson interferometer are equal. For higher currents, but yet below the threshold current, the amplified spontaneous emission causes the laser spectrum to be modulated by its cavity's longitudinal modes spacing.[7] In this case, peaks in the optical coherence tomography signal can be observed when the two arms of the Michelson interferometer differ by an integer multiple of $c/2f_{fsr}$.

A superluminescent diode, typically used in optical coherence tomography, generates light through amplified spontaneous emission. The reflectivity at its facets is minimized to prevent stimulated emission. Unlike a diode laser, its cavity's longitudinal modes cause much smaller modulations in its spectrum. The suitability of a superluminescent diode for optical coherence tomography is determined by the height of the principal peak occurring when the path difference is zero to the two small side peaks caused by the small modulation in its spectrum. These two side peaks are called secondary coherence subpeaks, and they should be negligible compared to the principal peak. They are observed when the optical path difference is c/f_{fsr}.[8]

Reference 1 uses the spectral width of a lasing longitudinal mode to directly calculate the reflectivity of the cavity mirrors to be $R = 0.994$, ignoring the gain and the loss within the cavity. The spectral width should be related to $Re^{(g-\alpha_{int})l}$ instead of R only. Here, g is the gain coefficient, and α_{int} is the internal loss coefficient, which has a value comparable to the mirror loss coefficient $\alpha_m = \ln(1/R)/l$.[4] Without knowing the gain and loss coefficients within the laser, it is impossible to estimate the reflectivity of the cavity mirrors correctly. Diode lasers have very high gain coefficients, and, usually, the uncoated laser cavity facets are sufficient.[5] The reflectivity can be found from the Fresnel reflection at the semiconductor–air interface for uncoated facets. For a typical refractive index $n = 3.2$, the reflectivity at the interface is $(n-1)^2/(n+1)^2 = 0.27$. Even with the gain and the internal loss ignored, the quoted reflectivity in Ref. 1 does not agree with Fig. 5. The width of the peak in radians is $4/\sqrt{F}$.[9] From the figure, the free spectral range is 14.3 GHz, and the full width at half maximum is 0.3 GHz, hence $2\pi \times 0.3/14.3 = 4/\sqrt{F} = 2(1-R)/\sqrt{R}$, which gives $R = 0.94$. To get $R = 0.994$, the width of the peak should be 0.026 GHz.

ACKNOWLEDGMENTS

This work was supported by the Deanship of Scientific Research at King Fahd University of Petroleum & Minerals under the Research Group Grant No. RG181004.

[a]Electronic mail: aljalal@kfupm.edu.sa, ORCID: 0000-0003-3967-2763.

[1]R. Poddar, S. R. Sharma, K. Bose, P. Sen, and J. T. Andrews, "A study of the longitudinal laser modes of a semiconductor laser using optical coherence tomography," Am. J. Phys. **75**, 569–571 (2006).
[2]J. J. ten Bosch and M. J. A. de Voigt, "Interferometric study of the modes of a visible-gas laser with a Michelson interferometer," Am. J. Phys. **34**, 479–482 (1966).
[3]A. F. Fercher, "Optical coherence tomography," J. Biomed. Opt. **1**, 157–173 (1996).
[4]G. P. Agrwal and N. K. Dutta, *Semiconductor Lasers* (Kluwer Academic Publishers, Amsterdam, 1993), pp. 34–238.
[5]O. Svelto, *Principles of Lasers* (Springer, New York, 2010), pp. 408–426.
[6]M. Moser, R. Winterhoff, C. Geng, I. Queisser, F. Scholz, and A. Dijrnen, "Refractive index of $(Al_xGa_{1-x})_{0.5}In_{0.5}P$ grown by metalorganic vapor phase epitaxy," Appl. Phys. Lett. **64**, 235–237 (1994).
[7]K. Möllmann, M. Regehly, and M. Vollmer, "Spectroscopy and microscopy analysis of semiconductor lasers in student laboratories," Eur. J. Phys. **41**, 025302 (2020).
[8]W. Drexler and J. Fujimoto, *Optical Coherence Tomography Technology and Applications* (Springer, New York, 2008), pp. 283–284.
[9]F. L. Pedrotti, L. M. Pedrotti, and L. S. Pedrotti, *Introduction to Optics* (Addison-Wesley, Boston, 2006), pp. 204–205.